Electric-Field-Induced Ion Evaporation from Dielectric Liquid

Manuel Gamero-Castaño*
Busek Co. Inc., 11 Tech Circle, Natick, Massachusetts 01760
(Received 23 May 2002; published 13 September 2002)

A direct proof of ion field evaporation from dielectric liquids is presented. The flux of sodium ions ejected from the surface of an electrospray of formamide is measured using time-of-flight and retarding potential techniques. The electric field at the emitting surface is varied through the electrospraying parameters. We find that the evaporated ion current is a very steep function of the electric field.

DOI: 10.1103/PhysRevLett.89.147602 PACS numbers: 79.70.+q, 47.65.+a, 82.80.Rt

The field evaporation of ions from a surface is a kinetic process driven by the presence of a repelling electric field. Ion field evaporation is known to occur from solids [1] and liquid metals [2]. This mechanism has also been invoked to explain the transfer of ions dissolved in dielectric liquids to the gas phase [3,4], although a demonstration of this phenomenon has proven to be extremely difficult. The confirmation of this process is important not only from a fundamental point of view, but also because of the role it plays in electrospray ionization, a technique that has revolutionized the field of mass spectrometry of proteins and other large biomolecules [5].

Support for the reality of ion field evaporation from dielectric liquids has been traditionally drawn from the study of the dry residues left behind by electrified nanodroplets, which presumably shed charge by this mechanism. Using standard aerosol techniques, the diameters and charge states of these residues have been measured and compared to the values derived from the assumption that ion field evaporation is acting [6,7]. The comparison between experiments and theory is quite good, and it is now accepted that (a) ion field evaporation from dielectric liquids does indeed occur naturally, and (b) it is the emission mechanism controlling electrospray ionization [8]. However, this type of demonstration is indirect in the sense that no evaporated ion currents are measured, nor is the electrification level of the liquid surface characterized. The reason for this stems from the difficulty of tracking a liquid nanodroplet while both its charge and liquid phase are evaporating. Fortunately, the nontrivial problem of measuring ion currents emitted from a steady surface of known electric field can be solved by studying electrosprays of dielectric liquids in the cone-jet mode. This geometry can become, under certain conditions, a steady ion-emitting surface [9]. The purpose of this Letter is to present this direct proof of ion field evaporation.

Figure 1 illustrates the typical geometry of a cone jet [10,11]. Liquid is fed to the tip of an electrified needle and, if the needle voltage and the flow rate are appropriate, the liquid shapes into a cone ended in a slender jet. Liquid and electric charge flow towards the end of the jet, which eventually breaks up into droplets. The cone region is quasi-fluid-electrostatic, because the cross section available for the transport of fluid and charge is large enough to accommodate the required conduction current and liquid flow rate with negligible voltage drop and fluid velocities. As the cone deforms into a jet, the quasistatic operation is no longer possible, charge is injected onto the surface, and the convected surface charge and bulk conduction current become comparable. Along the cone jet, the electric field reaches a maximum in this transition region, with a value given by [9]

$$E_J = \varphi(\varepsilon)\frac{\gamma^{1/2}K^{1/6}}{\varepsilon_0^{2/3}Q^{1/6}}, \tag{1}$$

where γ, K, ε, and Q are the surface tension, electrical conductivity, dielectric constant, and flow rate of the liquid, respectively, ε_0 is the permittivity of the vacuum, and $\varphi(\varepsilon)$ is a function of the dielectric constant with a value close to 1. As the fluid moves downstream from the tip of the cone, most of the current is transported as convected surface charge, and both charge and liquid are finally detached from the jet in the form of charged droplets. The electric field on the droplets is approximately given by [9]

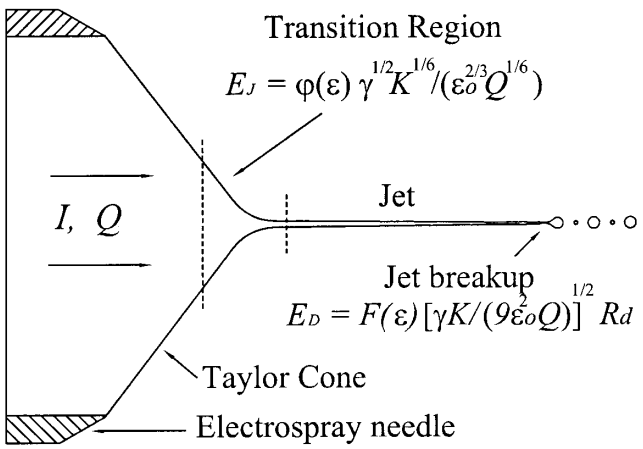

FIG. 1. Geometry of a cone jet.

$$E_D = F(\varepsilon)\left(\frac{\gamma K}{9\varepsilon_0^2 Q}\right)^{1/2} R_D, \qquad (2)$$

where $F(\varepsilon)$ is a function of order one [$F(\varepsilon) \cong 2$ for formamide, the liquid studied in this note], and R_D is the radius of the droplet. Using the scaling law for the mean droplet radius [10], we find that E_D and E_J scale similarly. Also note that, for a given solution electrosprayed at fixed flow rate, the larger droplets of the breakup distribution have larger electric fields.

In summary, there are two zones in the cone jet where the normal electric field exhibits maxima: the transition region and the larger droplets at the breakup. They are similar and controllable through the electrospraying parameters. For a given liquid, the electric field is increased by reducing the flow rate and/or by increasing the electrical conductivity. Cone jets of formamide seeded with sodium iodide evaporate ions at conductivity values of the order of 1 S/m. Under these conditions, typical jet diameters and electric fields are of the order of 10 nm and 1 V/nm [9].

The time-of-flight spectra shown in Fig. 2 illustrate the emission of ions and charged droplets. All the data reported in this Letter were obtained with the same solution of sodium iodide dissolved in formamide ($K = 1.69$ S/m at 25 °C). Each curve corresponds to a different flow rate, and the potential of the electrospray needle is 1546 V. The electrospray beam is directed towards a metallic collector, where the beam current, $I(t)$, is measured. At time equal to zero the potential of the needle is brought to ground, the electrospray is interrupted, and $I(t)$ diminishes as charged particles with similar velocities fully arrive at the collector. A more detailed description of this time-of-flight technique can be found in [12]. Going back to Fig. 2, note that every curve features two steps with different times of flight: the fastest step is associated with ions, and its time of flight is identical for every curve; i.e., the specific charge of the ions is independent of Q, as expected. The second step is due to charged droplets, which are known to have an increasing specific charge for diminishing Q. Clearly, the ions, having an acceleration voltage comparable to that of the droplets, are much faster because of their larger specific charge. Figure 3 compiles the previous time-of-flight data in the form of total electric current (ions plus droplets) and ion current, as functions of the liquid flow rate (the term "pl" stands for "picoliter"). As a reference, values of E_J are also given in the top x-axis; the unknown function $\varphi(\varepsilon)$ in (1) is taken to be unity. Note that for the larger flow rates, the ion current remains approximately constant, while the total current of the electrospray decreases with the flow rate following the well known scaling law $I \sim Q^{1/2}$ [10]. On the other hand, the ion current increases steeply below a critical flow rate, $Q^* \cong 46$ pl/s, $E_J \cong 1.02$ V/nm, and rapidly overwhelms the droplet current. Interestingly, the emission of ions at the lowest flow rates reverses the square root law for $I(Q)$, and the total current emitted by the cone jet increases for diminishing flow rates.

This phenomenology can be explained based on the field evaporation mechanism. As the flow rate decreases, the electric field on the cone-jet transition region increases, reaching in the proximity of Q^* values that promote a significant emission of ions. Additional small reductions on Q translate into large increments of the ion current, due to its exponential dependence on the electric

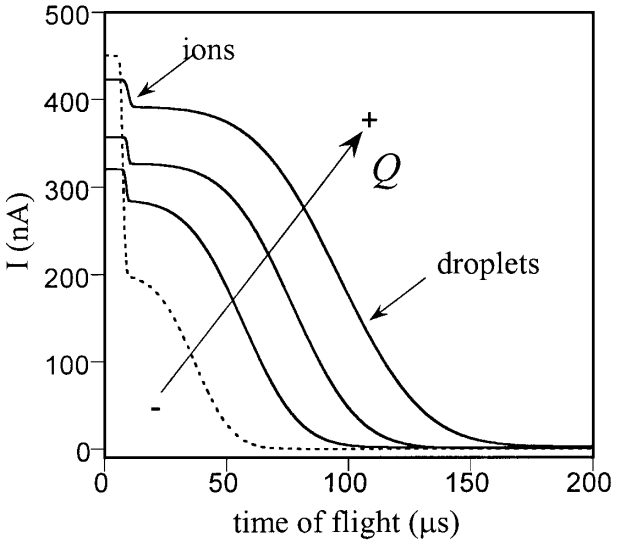

FIG. 2. Time-of-flight spectra showing ions and charged droplets.

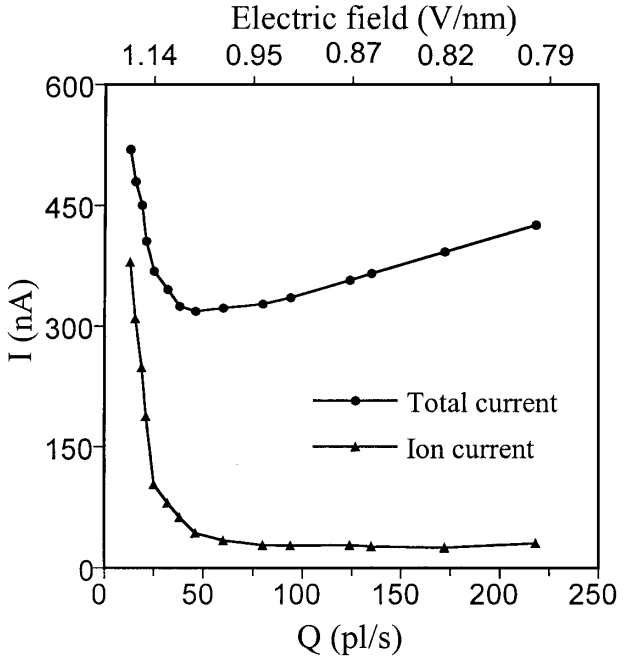

FIG. 3. Ion and total currents versus flow rate and electric field.

field [3]. The emission of ions from the transition region is also consistent with the reversing of the $I(Q)$ law: a large flux of ions can be transported to the surface of the transition region by conduction, where they are field evaporated, and the onset of this phenomenon changes the $I(Q)$ behavior. An increment of the total current for decreasing flow rates would not be possible if the ions were emitted only from the breakup, the other region where the electric field exhibits a maximum. The total current transported by the cone jet is fixed as convected surface current at the end of the transition region, and therefore the maximum current that could be evaporated from the breakup would be equal to that transported by the charged droplets, i.e., the square law for $I(Q)$ would still be fulfilled. On the other hand, ion evaporation from a few large droplets is compatible with the residual ion current at large flow rates observed in Figs. 2 and 3.

These ion emission scenarios can be confirmed with a combination of time-of-flight and retarding potential techniques. Measuring the retarding potential of the ions is important to establish whether they are evaporated from the transition region or from droplets, since there is a significant voltage drop along the jet [11,12]. We have used an experimental arrangement similar to that of [12], with the addition of three screens (grounded, connected to a retarding potential, and grounded) preceding the collector electrode (also grounded), and which are used to apply a voltage barrier. Thus, with this detector we can measure the time-of-flight spectra of the beam fraction with a retarding potential exceeding the voltage barrier. We also used an Einzel lens to correct the divergence of the electrospray beam. This allowed us to measure a significant fraction of the beam current with a relatively small collector positioned as far as 0.98 m from the electrospray source, and obtain the time of flight of the fast ions with improved resolution. Figure 4 shows time-of-flight spectra of the NaI-formamide solution at fixed flow rate and for different retarding potentials. The flow rate is 105 pl/s, within the high Q range in which the ionic emission is approximately constant (see Fig. 3). This figure shows that the retarding potential of every ion is smaller than that of a significant fraction of the droplets. Figure 5 plots the same type of spectra taken at a flow rate below Q^*. Although many ions and droplets disappear at relatively low retarding potentials, there is an important fraction of ions among the most energetic particles of the beam. Figure 6 represents the previous data as a function of the retarding potential, rather than time of flight. It contains the retarding potential curves of the overall sprays and the ionic fractions (defined as the ratio between the ion and the total currents). No time-of-flight measurement is necessary to obtain the retarding potential curve of the overall spray, only measuring the current arriving to the collector while sweeping the retarding potential is required. On the other hand, both time-of-flight and retarding potential measurements are necessary to obtain the ion fraction. Figure 6 shows that in the case of the higher flow rate, the ions are less energetic than the droplets. The low flow rate case is quite different: although ions and droplets are initially stopped at similar rates, there is a significant ion component characterized by having the highest energies in the beam. The retarding potential of a beam particle is written as

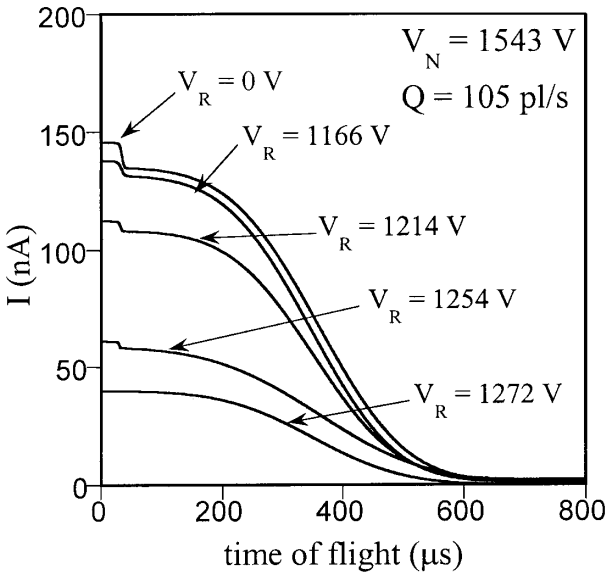

FIG. 4. Combined time-of-flight and retarding potential analysis at large flow rate.

$$V_R = V_E + \frac{1}{2}\frac{m}{q}v_E^2, \tag{3}$$

where V_E and v_E are the electrical potential and the velocity of the particle at the emission point, and q/m

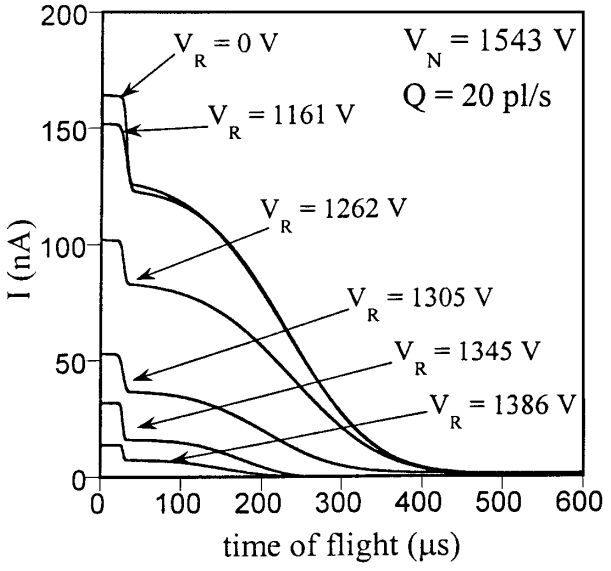

FIG. 5. Combined time-of-flight and retarding potential analysis at low flow rate.

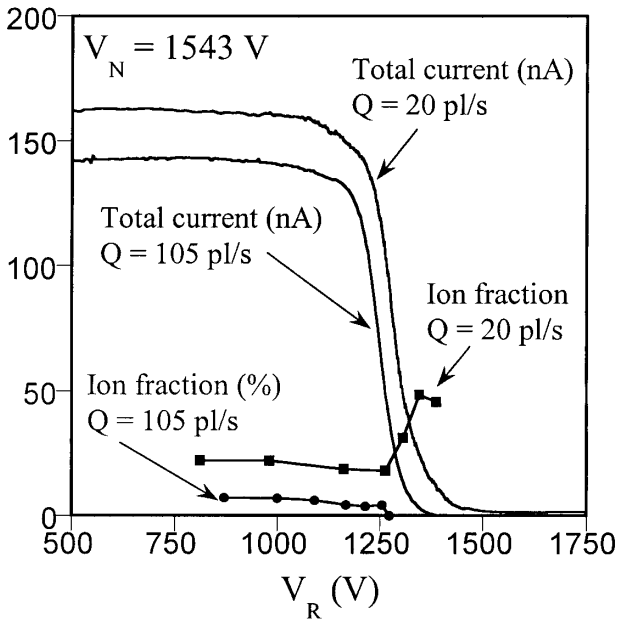

FIG. 6. Retarding potential distributions of electrospray beams and ionic fractions.

its specific charge. The emission voltages of all the ions emitted from the breakup region are similar, and smaller than the values associated with ions emitted from the transition region, since there is a voltage drop along the jet. This explains the two groups of ions with different energies observed in the spray at the lower flow rate. Note also that the retarding potential of the ions emitted from the breakup region must be smaller than the retarding potential of most droplets: while ions and droplets have similar V_E and ν_E (they both are emitted from the same region, and ion thermal velocities are significantly smaller than the fluid velocity), the specific charge of the ions is much larger than that of droplets. This is consistent with the results shown in Figs. 4 and 6 for the higher flow rate. Finally, it can be observed in the overall retarding potential curves of Fig. 6 that the emission of highly energetic ions from the transition region at the lower flow rate makes the lower section of the curve shift towards higher retarding potential values.

The mass of the ions is estimated from the time-of-flight and energy measurements. The most energetic ions at the lower flow rate, $Q = 20$ pl/s, have a mean time of flight of 27.7 μs, an acceleration voltage of approximately 1375 V, and the path of flight is 0.98 m. Thus, their mean specific charge and mass are 4.59×10^5 C/kg and 210 amu. Assuming that the ion is formed by a Na^+ core surrounded by a layer of formamide molecules, we get that the most common degree of solvation is 4.1 molecules of formamide. This value is similar to that found by Stimpson *et al.* [4]. These authors report that Na^+ ions emitted from glycerol have a continuous solvation degree spectrum with a distinct peak at 3 glycerol molecules. The larger solvation degree measured in our work is compatible with the smaller size of the formamide molecule and Bohr's model for a solvated ion.

In conclusion, we have shown that the electrospray mode referred to as cone jet provides a means to study directly the field-induced evaporation of ions from the surface of dielectric liquids. We have measured steady ion currents and the mass of the solvated ions; controlled and varied the electric field on the surface of the cone jet to evaporate ion currents of different magnitudes; and used time-of-flight and energy analysis techniques, along with our knowledge of cone jets, to explain the emissions of ions from these electrosprays.

I am indebted to Professor J. Fernández de la Mora for his guidance. I thank Dr. V. Hruby for his support.

*Email address: mgamero@busek.com

[1] E. W. Müller, Phys. Rev. **102**, 618 (1956).
[2] P. D. Prewett and G. L. R. Mair, *Focused Ion Beams from Liquid Metal Ion Sources* (Wiley, New York, 1991).
[3] J. V. Iribarne and B. A. Thomson, J. Chem. Phys. **64**, 2287 (1976).
[4] B. P. Stimpson *et al.*, J. Phys. Chem. **82**, 660 (1978).
[5] J. B. Fenn *et al.*, Science **246**, 64 (1989).
[6] I. G. Loscertales and J. Ferńandez de la Mora, J. Chem. Phys. **103**, 5041 (1995).
[7] M. Gamero-Castaño and J. Fernández de la Mora, J. Mass Spectrom. **35**, 790 (2000).
[8] P. Kebarle, J. Mass Spectrom. **35**, 804 (2000).
[9] M. Gamero-Castaño and J. Fernández de la Mora, J. Chem. Phys. **113**, 815 (2000).
[10] J. Fernández de la Mora and I. G. Loscertales, J. Fluid Mech. **260**, 155 (1994).
[11] A. M. Gañán-Calvo, Phys. Rev. Lett. **79**, 217 (1997).
[12] M. Gamero-Castaño and V. Hruby, J. Fluid Mech. **459**, 245 (2002).